The mitochondrial gene CMPK2 functions as a rheostat for macrophage homeostasis in inflammation.

Prabhakar Arumugam[1,2], Meghna Chauhan[1,2], Thejaswitha Rajeev[1], Rahul Chakraborty[1,2], Deepthi Shankaran[1,2], Sivaprakash Ramalingam[1,2], Sheetal Gandotra[1,2], Vivek Rao[1,2]*

1-CSIR- Institute of genomics and Integrative Biology, Mathura Road, New Delhi-110025 India.

2- Academy of Scientific and Innovative Research (AcSIR), Ghaziabad-201002, India

*Corresponding author: Tel: +91 11 29879229, E-mail: vivek.rao@igib.res.in

Running title: CMPK2 regulates macrophage inflammation

Key words: CMPK2, M1 macrophage, Immuno-metabolism, Mitochondria, infection

ABSTRACT:

Mitochondria, in addition to cellular energy production, are now being recognized as regulators of the innate immune response of phagocytes. Here we found that down regulation of the mitochondria associated enzyme, Cytidine Monophosphate Kinase 2 (CMPK2), results in a significant de-regulation of resting immune homeostasis of macrophages, presenting as an enhanced expression of the pro-inflammatory genes- IL1β, TNFα and IL8 in these cells associated with enhanced mitochondrial ROS and altered mitochondrial shape. Contrary to expectation, these phenotypic changes were also preserved in cells with constitutive over expression of CMPK2 thereby implicating an important role for this gene in the regulation of inflammatory balance of macrophages. Interestingly, long term modulation of CMPK2 expression resulted in increased glycolytic flux in both the silenced and over-expressing cells akin to the altered physiological state of activated M1 macrophages. While infection induced inflammation for restricting pathogens is regulated, our observation of a total dysregulation of basal inflammation by bidirectional alteration of CMPK2 expression, only highlights a critical role of this gene in mitochondria mediated control of inflammation.

Abbreviations: ROS- reactive oxygen species, IFN- Interferon, LPS-lipopolysaccharide, TLR-toll like receptors.

Introduction:

Eukaryotic cells are endowed with a versatile organelle- mitochondria that serves as an energy hub fueling cellular processes. The enormous metabolic flexibility offered by mitochondria resident processes forms the basis of cellular plasticity facilitating fine-tuned responses to physiological conditions[1, 2]. The importance of mitochondrial health in terms of physiology, network architecture in immune cell function and response to infection is well recognized[3, 4, 5]. Activated M1 polarized macrophages demonstrate an important shift in the metabolic state relying completely on glycolysis for increased and faster production of energy[5, 6, 7, 8, 9]. This transition is associated with a distinctive change in mitochondrial structure and a diminished reliance on mitochondrial oxidative phosphorylation and increased production of mitochondrial ROS[10, 11, 12, 13].

Intracellular infections compel host macrophages to activate selective cellular pathways to the inflammatory M1 profile of response resulting in activation of bactericidal pathways. The duality of the inflammatory response: controlling bacteria efficiently in a controlled fashion (host beneficial) to an extensive tissue damage on uncontrolled activation (detrimental) signifies the need to effectively regulate the onset and end of the inflammation. Several mechanisms have been defined for control of inflammation by host phagocytes [14, 15, 16, 17]. Studies in the last decade have implicated a determinant connection between mitochondria and the inflammation balance of immune cells [18, 19, 20]. With a central role of mitochondria in cellular metabolism and physiology, it is logical to presume stringent control of organelle integrity to achieve homeostasis even under stress. This necessitates high degree of flexibility in sense and response mechanisms of the immune cells.

We demonstrate that the mitochondrial resident kinase – CMPK2, is an important modulator of

inflammation in macrophages. CMPK2 is actively induced by infection in macrophages and responds primarily to TLR4 stimulation. Expression of CMPK2 is tightly regulated with a sharp increase in expression following infection of macrophages. Interestingly, macrophages with constitutively altered expression (stable silencing or over- expression) of CMPK2, demonstrated heightened levels of basal expression of inflammatory gene resembling the M1 macrophages. Concordant with this, we also observe a significant shift in macrophage metabolism to reliance on glycolysis and increase in mitochondrial ROS. A crucial role of regulated CMPK2 expression in controlling bacterial growth effectively provides an important link between mitochondrial metabolism and innate response kinetics of macrophages.

Results:

Macrophages respond to infection/ TLR4 stimulation by inducing *CMPK2*.

A well-orchestrated transcriptional response is initiated in macrophages infected with intracellular and extracellular bacteria. With type I IFN as one of the earliest responses of infected macrophages [21, 22, 23], it was not surprising that the interferon stimulated gene (ISG)- *CMPK2* also showed significant increase in expression following Mtb infection. Infected macrophages showed a steady increase in *CMPK2* expression from 15-fold of expression by 6h and attaining peak levels of ~140 fold by 12h and thereafter maintained to greater than 100- fold even at 24h of infection (Fig. 1A). In line with previous reports [24], we also observed nearly 20- fold increase in *CMPK2* expression in response to LPS stimulation while the other TLR ligands failed to alter this gene (Fig. 1B). This was also evident as a steady increase in CMPK2 protein levels in THP1 macrophages even at 48h of LPS stimulation (Fig. 1C). The complete loss of LPS induced expression in the presence of a TLR4 signaling inhibitor-CLI095, confirmed the dependence of *CMPK2* expression on TLR4 signaling in macrophages (Fig. 1D). Further, macrophages responded to *Salmonella enterica subsp. enterica serovar* typhimurium (STM) infection, by early induction of *CMPK2* expression with 15-16 -fold increase by 3h wherein escalated further to ~30 fold by 6h of infection (Fig. 1E) and this response was completely abolished with the addition of

CLI095 confirming the TLR4 dependent expression of this gene in macrophages (Fig. 1F). A decrease in expression by more than 50% was observed in the case of macrophages infected with Mtb and treated with CLI095 again supporting the importance of TLR4 signaling in *CMPK2* expression (Fig. S1).

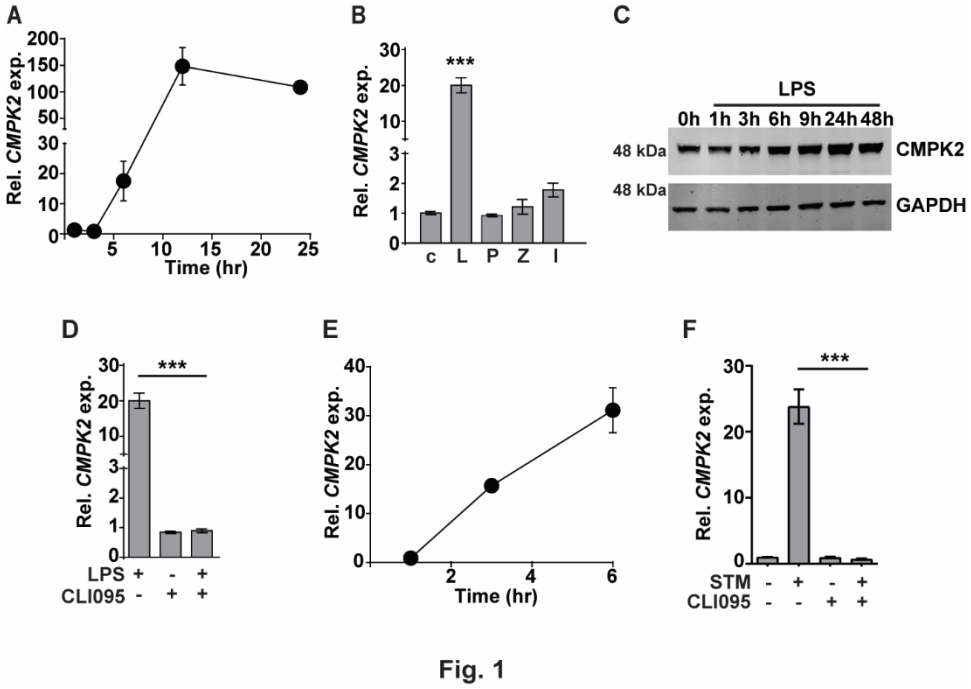

Fig. 1: CMPK2 expression in macrophages following stimulation.

[A-F] Analysis of CMPK2 expression in THP1 macrophages following: infection with Mtb at a MOI of 5 [A], stimulation with various TLR ligands- c: Untreated cells**,** L: LPS (10 ng/ml), P: Pam3CSK4 (20 ng/ml), Z: Zymosan (10 µg/ml), I: Poly IC (2 µg/ml) [B], LPS stimulation by immunoblotting with CMPK2-specific antibody [C], LPS stimulation with and without TLR4 inhibitor CLI095 [D], infection with STM [E], infection with STM in the presence of CLI095 [F]. Expression of *CMPK2* was quantitated by qPCR. Values are normalized with *GAPDH* and mean fold change compared to control cells $\pm$ SEM from N=2/ 3 independent experiments.

Modulation of CMPK2 activity affects the inflammation status of macrophages.

In order to decode the molecular function of CMPK2 in the macrophage response, we used *CMPK2* specific siRNAs (a-c) to specifically silence this gene in THP1 cells (CM) and achieved

60-75% decrease in gene expression in comparison to scrambled siRNA (SC) (Fig. S2A). Only siRNA-c showed a significant dip in protein levels in excess of 40% of the native CMPK2 expression and was used for further analysis (Fig. 2A). Given a critical role of proinflammatory cytokines in macrophage response to infection, we compared the levels of TNFα and IL1β in the SC and CM macrophages in response to Mtb infection. Mtb infection induced *TNFα* and *IL1β* expression by 100-150- fold in CM macrophages while these levels were 3-4- fold lower in the case of SC macrophages (Fig. 2B). Interestingly, expression levels of these genes were markedly elevated in the uninfected cells. This pattern was also reflected by the enhanced expression levels of other immune effectors like *IL8*, *IP10*, *VEGF* and decrease in *IL10* in naïve CM macrophages strongly alluding to an enhanced pro- inflammatory status of these cells even in the resting state (Fig. 2C). This profile of increased *TNFα* and *IL1β* gene expression was observed in CM cells following LPS stimulation (Fig. S2B). This enhanced expression also correlated well with the increase in secreted TNFα and IL1β in the culture supernatant of LPS treated CM cells (Fig. 2D). Again, correlating with gene expression, naïve CM cells also secreted increased amounts of both TNFα and IL1β in the supernatants as compared to the non- detectable levels of the cytokine in naïve SC macrophages.

Given the inflammatory phenotype observed with decreased CMPK2 expression in THP1 macrophages, we attempted to reverse this by complementing a functional copy of the gene in the silenced cells. We expressed the complete CMPK2 as a mCherry fusion protein in pCDNA3.1 and analyzed the basal expression levels of *IL1β* and *TNFα*. As expected, *CMPK2* expression was ~30 folds higher levels than in empty vector control THP1 cells (Fig. 2E). Contrary to our expectations, this enhanced expression of the *CMPK2* could not reverse the alteration in basal inflammation of these cells: nearly similar levels of *IL1β* and *TNFα* was observed in the complemented cells as in the silenced cells (Fig. 2F). We hypothesized that similar to the situation with CMPK2 silenced cells, increase in expression of CMPK2 was also detrimental to the inflammation homeostasis of macrophages. To test this, we analyzed the pro inflammatory status

of THP1 cells stably expressing CMPK2-mCherry. Enhanced expression of *CMPK2* transcript in excess of 100- fold basal levels was observed in the over expressing (OE) cells (Fig. S2C). The fusion protein of CMPK2 and mCherry was also clearly detected in protein extracts of the OE strains by immunoblotting (Fig. S2D). Again, this enhanced expression of CMPK2 resulted in heightened levels of *TNFα* (12-15- fold) and *IL1β* (100-150- fold) in OE cells (Fig. 2G).

In an effort to understand the basis for the hyper-inflammatory state of CM and OE cells, we compared the immune signaling cascades of these cells with the respective controls in the basal state. Consistently, we observed enhanced activation of ERK and NFκB with 3-fold higher level of phospho-p42-44 ERK and p65 NFκB (Fig. 2H, S2E) without any change in p- JNK and p38 MAP kinase in CM cells compared to SC cells (Fig. S2F). This pattern of enhanced ERK phosphorylation was also observed in the case of OE cells in comparison to VC cells. The use of an ERK signaling specific inhibitor U0126 not only reduced the levels of p42-44-ERK in both the CM and OE cells (Fig. 2I), but also significantly reduced the elevated levels of both *IL1β* and *TNFα* in both these cell types, further confirming the importance of ERK signaling in mediating the hyper inflammatory phenotype of these macrophages (Fig. 2J, 2K).

Human mitochondrial CMPK2 has been shown to be a nucleotide kinase involved in mitochondrial DNA synthesis (Fig. 2L). In an effort to probe the importance of the kinase domain, we substituted the active site aspartate to alanine (D330A) as a kinase dead variant of CMPK2 (D330A) and analyzed the functional consequence of this expression on cytokine gene expression. Despite the strong and stable expression of D330A, comparable to the Wt CMPK2 (OE), both at the transcript (Fig. S2G) and protein (Fig. 2L) level, there was no evidence of increased basal inflammation. Contrasting with the significantly elevated levels of *TNFα* and *IL1β* in the OE cells (~10 and ~80 fold, respectively over basal levels), THP1 cells transfected with D330A, harbored normal levels of gene expression (Fig. 2M) emphasizing the importance of the kinase activity of CMPK2 in regulating basal inflammation in macrophages.

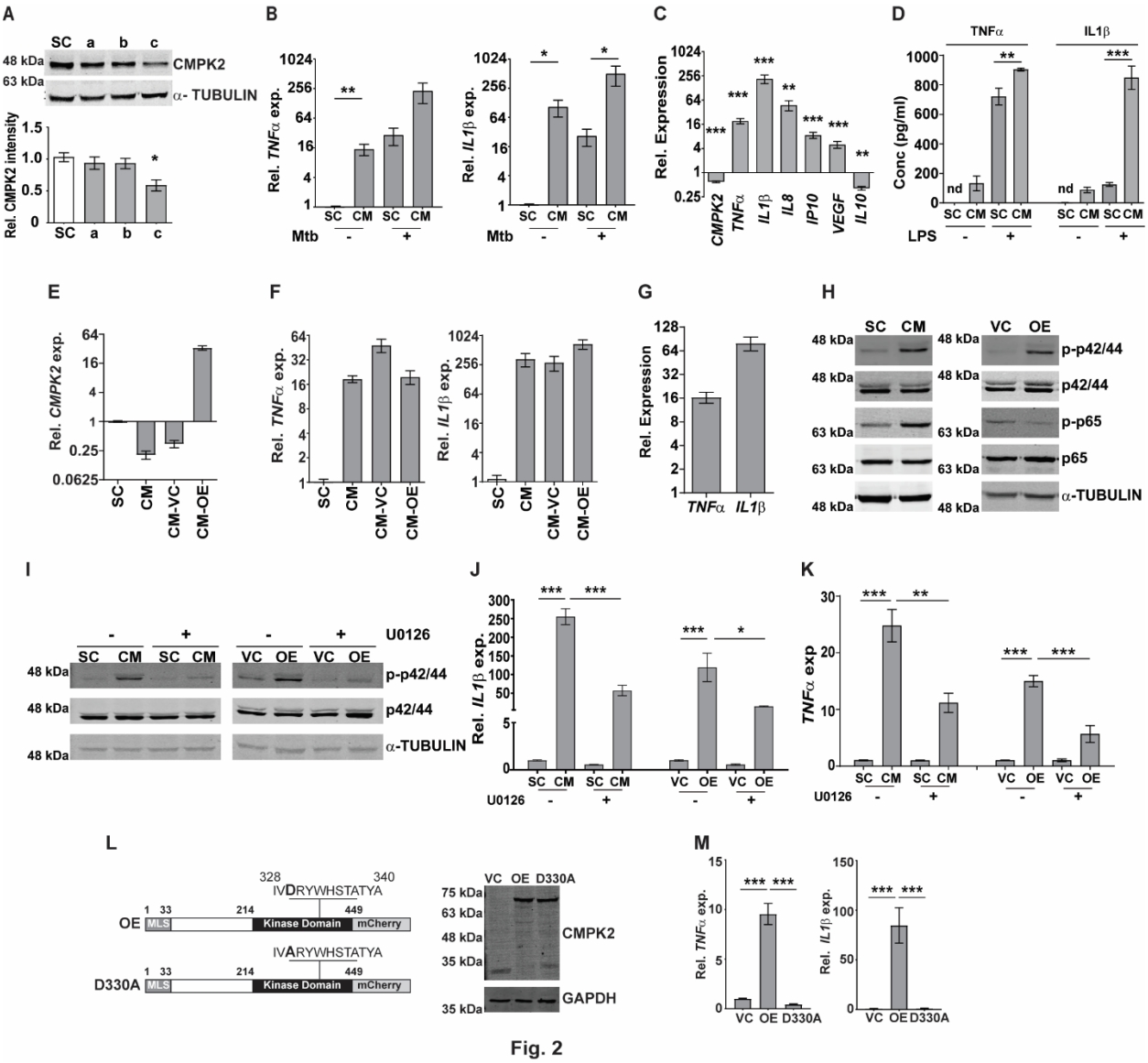

Fig. 2: CMPK2 regulates the basal inflammation of macrophages.

[A] Expression of CMPK2 in CMPK2 silenced macrophages by immunoblotting with specific antibodies. For immunoblotting, the expression of α-TUBULIN was used as control. One representative blot of 3 independent experiments is shown. The levels of CMPK2 expression are depicted as mean fold change ± SEM of N=3 experiments by densitometry. [B] Expression of the *IL1β* and *TNFα* transcripts following infection with Mtb for 6h was evaluated in SC or CM macrophages by qPCR. [C] Basal level expression of transcripts *CMPK2* and cytokine genes in CM macrophages was estimated by qPCR with specific primers. Values are normalized with GAPDH and mean fold change compared to control cells ± SEM from N=3

independent experiments. [D] Levels of TNFα and IL1β in the culture supernatants of THP1 stably expressing scrambled (white bars) or siRNA specific to CMPK2 (grey bars) estimated by ELISA. Values are represented as mean pg/ml of the cytokine in triplicate assays from N=3 experiments. E] Expression of *CMPK2* in the CMPK2 silenced cells with stable expression of CMPK2 (CM-OE) or empty vector (CM-VC). The levels in the corresponding SC and CM cells are also shown. Values are represented as mean ± SEM of the triplicate assays from N=3 experiments. F] Expression of *TNFα* and *IL1β* in the CMPK2 silenced cells with stable expression of CMPK2 (CM-OE) or empty vector (CM-VC). The levels in the corresponding SC and CM cells are also shown. Values are represented as mean ± SEM of the triplicate assays from N=3 experiments. G] Expression of *TNFα* and *IL1β* in THP1 cells after stable expression of CMPK2. Values are represented as mean ± SEM of the triplicate assays from N=3 experiments. H] Analysis of activation of the ERK (p42/44) and NFκB (p65) signaling pathways in SC, CM, VC and OE macrophages by immunoblotting with antibodies specific for the phosphorylated (active) and non- phosphorylated forms of the proteins. Representative blot of one experiment out of 3 individual assays is shown. Expression of α-TUBULIN was used as control. I] ERK phosphorylation in macrophages with and without treatment with ERK specific inhibitor U0126. Antibodies specific for the phosphorylated (active) and non- phosphorylated forms of the proteins were used to probe cell extracts. Expression of α-TUBULIN was used as control. Blots are representative of two independent experiments. J-K] Expression of *IL1β* (J) and *TNFα* (K) in the 4 types of macrophages after treatment with U0126 was analyzed by qPCR. Cells left untreated were used as control. The relative gene expression folds in triplicate assay wells are represented with respect to GAPDH as mean ± SEM for N=2. L] The schematic of mutated catalytic site also depicted (D330A). Immunoblot analysis of CMPK2-mCherry fusion protein using antibody specific for mCherry protein in protein lysates of VC, OE and D330A THP1 cells with mCherry specific antibody. GAPDH was used as control. M] Expression of *TNFα* and *IL1β* in THP1 cells after stable expression of vector alone (VC) full length CMPK2 (OE) and catalytic mutant of CMPK2 (D330A). The relative gene expression folds in triplicate assay wells are represented with respect to *GAPDH* as mean ± SEM for N=4.

Increased inflammation of CM macrophages is associated with altered mitochondria and augmented ROS.

We presumed that identifying the precise localization of CMPK2 would reveal clues to its molecular role in inflammation and mitochondrial membrane dynamics. We first validated the mitochondrial localization of CMPK2 by immunoblotting subcellular fractions. With previous reports indicative of a mitochondrial localization of CMPK2[25] and our observation of a majority of the protein in the mitochondrial fraction (Fig. 3A), we tested purified mitochondrial fractions to pinpoint its location by standard biochemical and immunoblotting analyses. While treatment with Proteinase K (removes the surface exposed proteins), completely removed the outer membrane protein TOM20, nearly 30% of CMPK2 was present in the pellet fraction of intact mitochondria, similar to that observed for the other mitochondrial membrane associated protein –TIM50 (Fig. 3B) suggesting its association with the outer membrane of mitochondria. Most of the matrix protein- SOD2 remained in the pellet and was lost only with complete solubilization with Triton X-100. The peripheral association of CMPK2 with the mitochondrial membrane was also revealed by a relatively higher amount of CMPK2 in the soluble fraction of mitochondria treated with Na_2CO_3 in contrast with the integral membrane protein- TOM20 (Fig. 3C).

We hypothesized that two distinct possibilities could account for the enhanced basal levels of inflammation observed in the CM and OE lines - 1) enhanced expression at all times or 2) a temporal activation of the signaling with delayed decay kinetics. To test this, we checked the expression of IL1β in the two cell lines during the monocyte to macrophage transition upon PMA treatment. While the monocytes did not show any difference in IL1β expression, activation with PMA induced distinct profiles of IL1β activation in the control (SC) or CMPK2 silenced (CM) cells. A rapid increase in IL1β within a day of activation (~700 fold) was followed by a steady decline by 72h of treatment further reaching basal levels by day 4 in the control cells (Fig. 3D). CMPK2 silenced macrophages, however, displayed a protracted response kinetics with a slower rise in expression levels ~1.5-2 folds lower than control cells at 24 h of activation with PMA. Between 24h and 72h of treatment, the levels were 3-5 fold higher in CM with a delayed decline of the levels to ~500 fold by day 4 and did not fall to basal levels even by day 5.

Macrophage inflammation is strongly associated with ROS activation. To check this, we compared the levels of mitochondrial ROS in SC and CM macrophages by using a ROS specific stain- MitoSOX Red. Mitotracker deep red was used as control for the levels of mitochondria in the two cell types. While similar levels of mitotracker staining hinted at unaltered mitochondrial levels, the level of ROS (mitosox) was nearly 1.5-fold higher in CM cells as compared to control SC macrophages (Fig. 3E). The importance of mito- ROS in enhanced inflammation in CM cells was further evident when the cells were treated with a specific inhibitor- mitoquinone (MQ). Addition of MQ early (immediately after PMA treatment) significantly reduced the expression of IL1β in these cells (Fig. 3F); use of MQ at later stages of differentiation (48h and 72h after PMA addition) did not alter the inflammation in the CM cells (Fig. S3A, B). Mitochondrial membrane polarization is a critical component of organelle integrity and physiology with alterations in membrane potential leading to ROS in macrophages[26, 27]. To test if the ROS was associated with change in membrane potential, we compared the extent of TMRE staining (a dye that shows a potential dependent differential partitioning across mitochondrial membranes) in the SC and CM cells. As seen in Fig. 3G, the mitochondria of CM macrophages exhibited significantly lower staining with TMRE, similar to the SC cells treated with the proton pump uncoupler- CCCP, suggestive of a loss of membrane integrity in the latter cells even at the basal level. CCCP further decreased the mitochondrial membrane potential of the CM cells.

In order to test if the altered membrane potential affected mitochondrial architecture, we compared the morphology of these organelles in the SC, CM, VC and OE cells. In sharp contrast to the small uniformly distributed mitochondria in the control cells (SC and VC), larger and more dense mitochondrial network was observed in the CM and OE cells (Fig. 3H, 3I). Mitochondrial architechture and function is strongly dependen on the relication dynamics of these organelles. Evaluation of the mitochondrial fission- fusion (replication) dynamics in the 4 cell types revealed an important role for CMPK2 in regulating this process. Both in CM and OE cells, the levels of DNM1L (crucial for mitochondrial fission) was expressed at 1/3rd the level observed in the SC and

VC cells (Fig. 3J) contarsting with an unaltered expression of the mitochondrial fusion associated proteins (MFN1 and OPA1) in these cells (Fig. S3C, S3D) implying the importance of optimal CMPK2 expression in mitochondrial physiology.

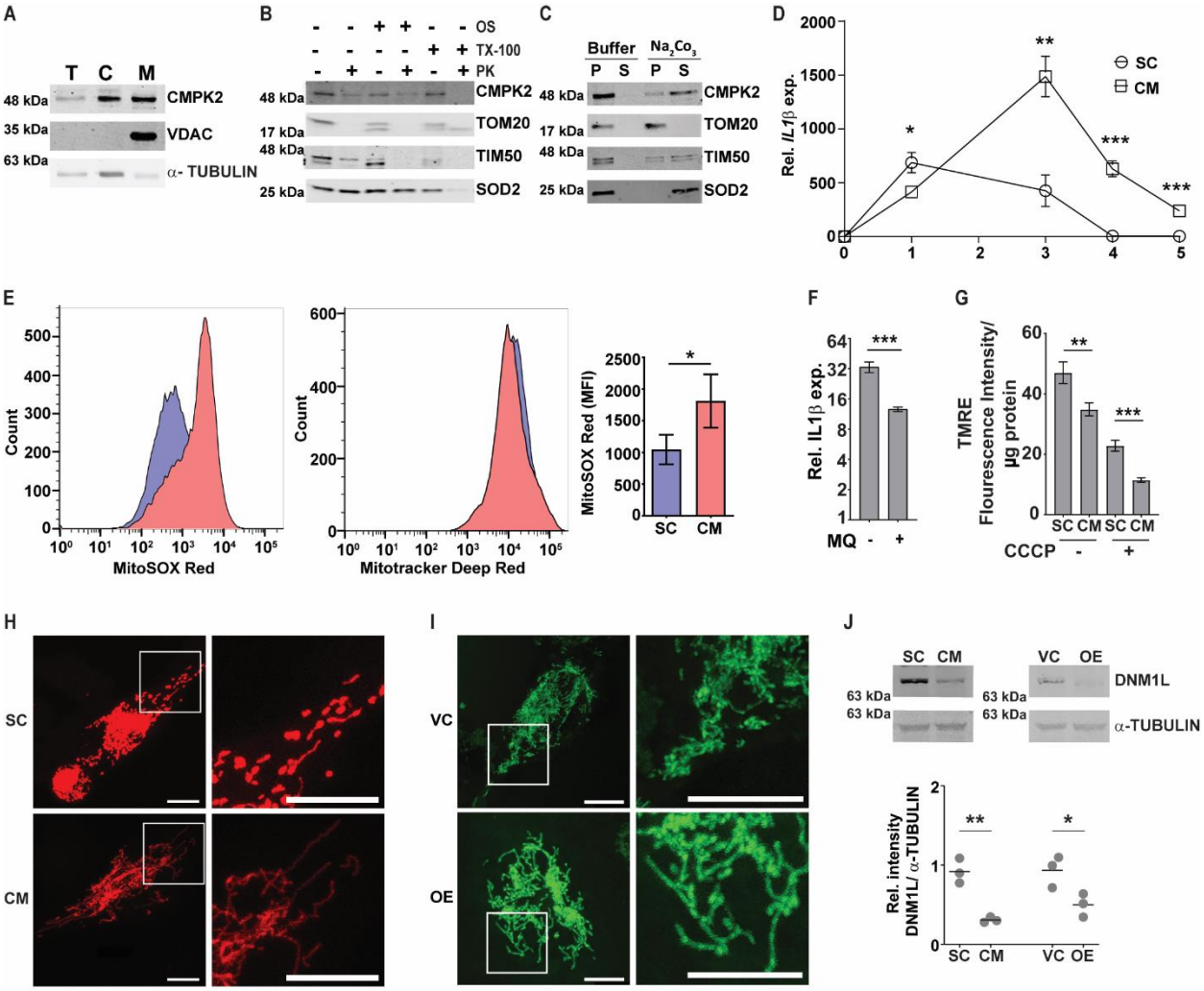

Fig. 3

Fig. 3: Modulation of CMPK2 affects the mitochondrial physiology in macrophages.

A] Expression of CMPK2 in subcellular fractions of THP1 macrophages by immunoblotting with specific antibodies, T- total cell extract, C- cytoplasmic fraction and M-Mitochondria. Expression of cytosolic protein α-TUBULIN and mitochondria resident protein VDAC are also represented. Blots are representative of three independent experiments. B] Mitochondrial fraction was subjected to Proteinase K treatment in the presence or absence of Triton X-100 and given osmotic shock (OS) and analyzed by immunoblotting. Data are representative of three independent experiments. C] Mitochondrial fraction was incubated with

mitochondrial buffer with and without Na_2CO_3 and centrifuged at 13,000 rpm for 15 min. The pellet (P) and supernatant (S) factions were immunoblotted. Data are representative of three independent experiments. D) Kinetic profile of *IL1β* expression in SC and CM during differentiation of monocytes to macrophages. Expression was checked at different time intervals after PMA treatment. Values are mean fold change in expression with respect to *GAPDH* ± SEM triplicate assays of N=2 experiments. E) Analysis of mitochondrial ROS in SC or CM macrophages. Cells were stained with MitoTracker Deep Red (as an internal control) and ROS specific MitoSOX Red and specific population were quantified by FACS. The histogram plots of a representative experiment of (N=4) is depicted. The extent of MitoSOX red mean fluorescence intensity (MFI) ± SEM is represented graphically in the inset. F) Expression of *IL1β* in the macrophages with the addition of a specific mitochondrial ROS inhibitor- MQ at day1 of PMA treatment was analyzed by qPCR. Values are mean fold change in expression with respect to *GAPDH* ± SEM for triplicate assays of N=3 experiments. G] Analysis of mitochondrial membrane potential in SC or CM macrophages by TMRE staining. Fluorescence values normalized to protein in samples is represented as mean fluorescent intensity ± SEM for triplicate assays of N=3 experiments. H, I] Mitochondrial architecture in THP1 macrophages upon silencing CMPK2. Macrophages with control (SC) or CM [H] or VC or OE [I] was analyzed by confocal microscopy. A representative image is depicted with the scale bar representing 10μM, the region shown in higher magnification is depicted with the box. J] Expression of gene involved in mitochondrial fission by immunoblotting with specific antibody. Expression of DNM1L is depicted along with α-TUBULIN levels as a control. Relative intensity values are depicted as mean± SEM of N=3.

Regulated levels of CMPK2 is critical for the normal metabolic activity of macrophages.

In an attempt to understand the basis for this dysregulated inflammatory gene expression in both the CM and OE macrophages, we performed global sequencing of transcripts and compared the expression profiles with the control macrophages -SC and VC, respectively. Strikingly, again, on comparison of the differentially expressed genes, inflammatory cytokine genes like IL1β, IL8, TNFα were commonly upregulated in both the CM and OE macrophages (Fig. 4A). This consistency in gene expression profiles was also evident with the significantly large numbers of genes increased (515) or decreased (500) in macrophages with abnormal CMPK2 expression

(Fig. 4A inset). A significant deregulation of basal level inflammation was also evident in Gene Set Enrichment Analysis (GSEA) with heightened inflammation response as a key gene family common to the two macrophage lines (Fig. 4B). Interestingly, enhanced expression of the hypoxia genes combined with the higher inflammatory profile was reminiscent of M1 activated macrophages. To validate this, we analyzed the expression profiles of previously identified signatures of M1 and M2 polarized macrophages in our genesets[28]. In agreement to our hypothesis, both the CM and OE macrophages showed increase in the expression of genes of M1 macrophages with a majority of the M2 specific signatures either unchanged or with reduced expression levels (Fig. 4C). Further validation of a M1 bias was visible in the physiological state of the cells. A deeper analysis revealed an increase in the expression of genes involved in glycolysis (Fig. S4A, S4B) that manifested as a significant increase in the levels of glycolysis intermediates like glucose / fructose 6-P, fructose bis-phosphates, DHAP, culminating in markedly high levels of lactate (Fig. 4D). The associated decrease in genes and metabolites of the TCA cycle was further supportive of a strong proinflammatory M1 like phenotype of both the CM and OE macrophages. Moreover, both these cell types (CM and OE), displayed a significant reduction in the NAD/ NADH ratios on account of significantly higher levels of NADH in the two cell types with a 1.5-fold increase in net ATP levels in the CM cells (Figs. 4E, 5F). Further, analysis of respiration rates of cells revealed a distinct pattern with a considerable dip in the oxygen consumption rates of macrophages with altered expression of CMPK2. Both the CM and OE macrophages displayed 2-2.5 folds lower oxygen consumption with delayed kinetics as opposed to the control macrophages SC and VC (Fig. 4G, H) implicating a strong shift of macrophages with altered CMPK2 expression towards a pro-inflammatory phenotype and the important role for CMPK2 in maintaining homeostasis of macrophages.

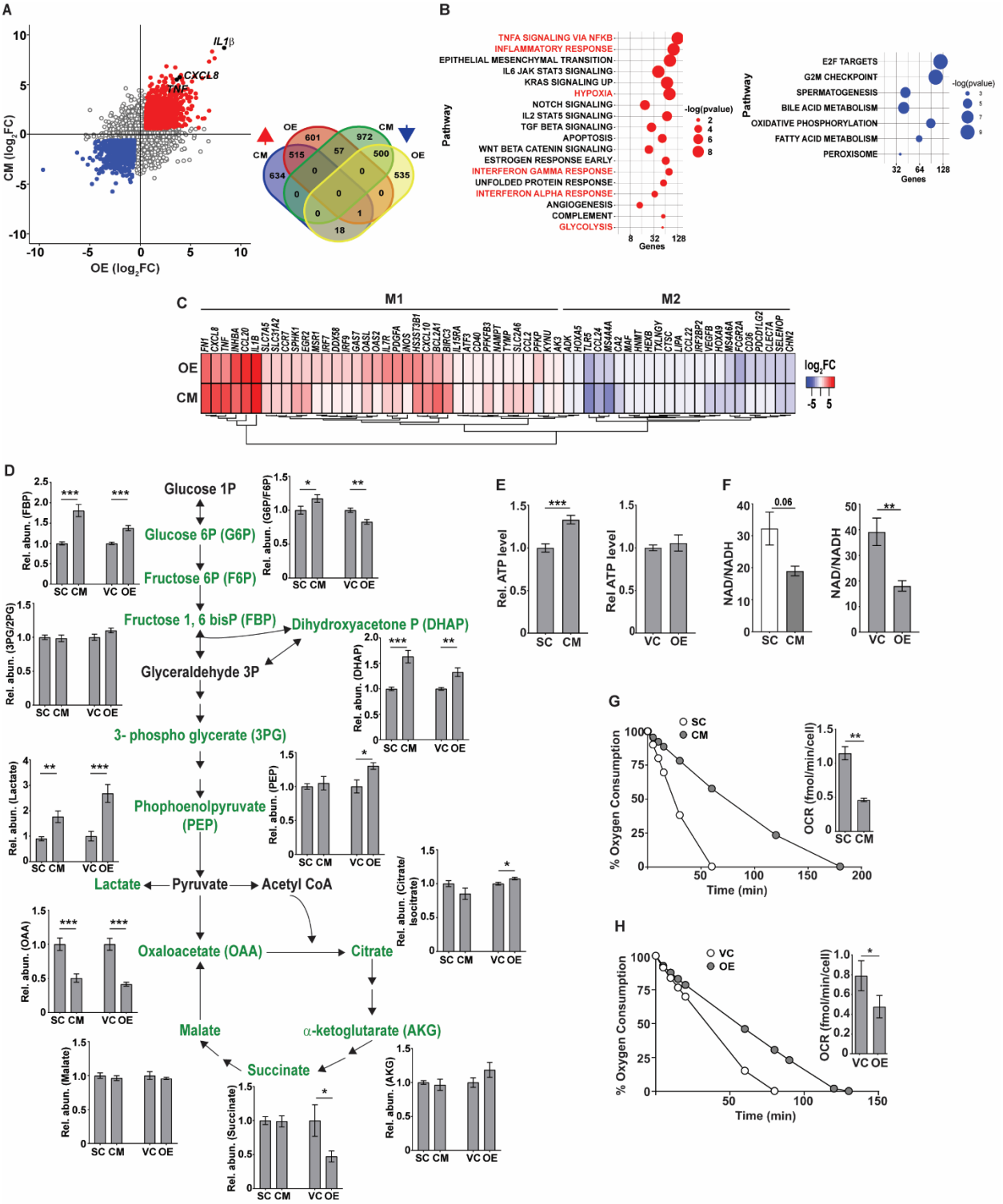

Fig. 4

Fig. 4: Macrophages with dysregulated CMPK2 display inflammation and metabolic signatures of activated M1 macrophages.

A) Scatter plot of genes differentially expressed in CM or OE macrophages relative to the expression levels in the control macrophages (SC or VC), respectively. Change in expression is depicted as $\log_2$ fold change in expression. The number of genes up- and down- regulated in the macrophages are depicted as a Venn diagram (inset). B) GSEA hallmark pathway enrichment analysis of the commonly up and down regulated genes in the CM and OE macrophages are represented as a bubble plot. X axis is the number of genes of the pathway and size of the bubble depicts significance (-log P value). C) The expression patterns of genes specific to M1 and M2 activated macrophages in the CMPK2 dysregulated macrophages CM and OE are represented as heat maps. The values represent $\log_2$ fold change from the corresponding control cells. D) Metabolite levels in the CMPK2 silenced (CM) and over-expression (OE) and their respective control macrophages were assayed from cellular extracts by MS. The levels of individual metabolites in the CM and OE macrophages (represented in green) are represented as relative percent of the concentrations in the respective control cells as mean $\pm$ SEM from 3 independent experiments (N=3). E&F) The levels of ATP (E), NAD, NADH (F) in the different macrophages was determined by MS. The relative levels of ATP or the ratio of NAD and NADH are represented as mean values $\pm$ SEM in the CMPK2 modulated cells with respect to the control cells of N=3/2 experiments. G&H) Continual estimation of oxygen consumption in SC, CM (G) and VC, OE (H) macrophages until 3h with Oroboros oxygraph. The level of oxygen consumption was calculated and mean OCR values $\pm$ SEM of N=3 experiments is shown in the inset.

CMPK2 plays a critical role in the macrophage ability to control infection

To understand the impact of altered CMPK2 expression in macrophage inflammatory properties, we evaluated its ability to control intracellular growth of Mtb. We observed a 2-3 fold decrease in intracellular bacterial numbers in these macrophages as compared to SC late in infection (day 5), CM cells were able to control bacterial levels to input levels by this timepoint compared to growth of about 5-6 folds in the SC macrophages (Fig. 5A). This pattern of increased bacterial control was also evident in STM infected CM macrophages with 2-3 fold lower bacterial numbers after 24 h of infection (Fig. 5B).

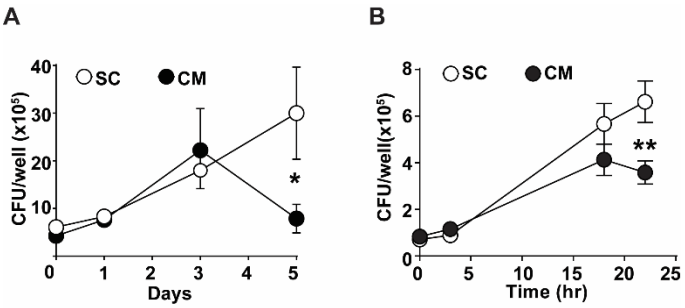

Fig. 5: CMPK2 regulates bactericidal activity of macrophages

A] Growth kinetics of Mtb in SC and CM macrophages at different times post infection at a MOI of 5 for 6h. Values are mean CFU ± SEM values in triplicate assays of N=4. [B] Growth kinetics of STM in SC and CM macrophages at different times post infection at a MOI of 10 for 20 min. Values are mean CFU ± SEM values in triplicate assays of N=4.

DISCUSSION

Macrophages, the primary cells that sense and respond to any infectious agents or tissue damage, are critical components of vertebrate innate immune responses. Being endowed with the capacity to initiate and manifest strong infection control programs to a variety of pathogens, they often dictate both acute and chronic outcomes of infection in the host[29, 30]. Recent evidence implicates these cells in maintenance of tissue homeostasis during steady state and inflammation[30, 31, 32, 33]. Apart from controlling the infection response, they are actively involved in removal of cellular or bacterial debris to prevent long term inflammation[33, 34, 35]. Several studies have identified functionally distinct macrophage sets with polarized pro-inflammatory (M1) or anti-inflammatory (M2) phenotypes with distinct metabolic characteristics[36, 37, 38]. An important role for mitochondrial dynamics and function is recognized in regulating host cell metabolism as well as the response to infections[39, 40]. Several stimuli or bacterial infections modulate mitochondrial function in order to influence immune signaling[10, 41, 42]. Contrasting with the glycolytic shift in cellular metabolism in response to LPS stimulation or infection in the M1 polarized macrophages, IL4 induced M2 macrophages predominantly rely on oxidative phosphorylation and fatty acid

oxidation for energy[43, 44] thereby implicating the mitochondria in regulating macrophage immunometabolism.

We provide evidence for an important role of the mitochondrial gene CMPK2 in regulating the basal inflammation in human macrophages. CMPK2 has previously been identified as a dominant component of macrophage anti-viral response to HIV, DENV, SVCV [25, 45, 46, 47]. Recently, CMPK2 has been shown to be involved in regulating foam cell formation in artherosclerosis[48]. Mouse CMPK2 has been shown to be involved in the synthesis of mitochondrial DNA and is critical to the formation of ox-mtDNA fragments in response to NLRP3 activation [24] implicating this gene in regulation of innate immune response. However, the exact function of CMPK2 is still unclear. To elucidate a role of CMPK2 in macrophage physiology, we tested the effect of CMPK2 silencing as well as over expression and demonstrate gross changes in the inflammatory capacity, orienting cellular metabolism towards rapid energy production via glycolysis to facilitate a pro-inflammatory M1 phenotype in the macrophages. Macrophages with altered CMPK2 levels (CM and OE) show consistent features of enhanced activation of ERK signaling leading to a marked increase in production of pro- inflammatory mediators like TNFα, IL8, IL1β dependent on the manifestation of increased mitochondrial ROS.

These conditions mimic the strong induction of CMPK2 in macrophages following infection by intracellular bacteria like STM or Mtb, thereby preparing cells for M1 polarization required for infection control [49]. Given our observation of similar phenotypes in both gene silenced and over expression cells, it is logical to assume the association of CMPK2 in a larger protein complex in cells[50]. In support of this, we found this protein to localize to the mitochondrial membrane suggesting its proximity to the mitochondrial ETC proteins. In fact, we also observed a decrease in levels of complex 1 (Fig. S5), lending further credence to an impaired oxidative phosphorylation in these cells. This was also supported by the severe impairment in oxygen consumption with a concomitant increase of the glycolytic metabolite- lactate in the CM and OE macrophages.

Recently, lactate production by M1 polarized macrophages has been attributed to microbicidal capacity of these cells against Mtb[51].

We observed that removal of MLS from CMPK2 destabilized the protein and resulted in enhanced degradation by the cellular proteolytic machinery. This observation is in sync with previous reports[52] demonstrating that mitochondrial proteins without signals for mitochondrial partitioning tend to form mis-folded aggregates that are rapidly degraded by the host proteasome [53]. We also observed an absolute requirement of kinase activity for CMPK2 function and the importance of the N- terminal DUF domain in protein stability (data not shown, part of another manuscript).

Given the importance of CMPK2 in maintaining mitochondrial architecture, function and in enhancing overall inflammation, macrophage would actively induce this gene as a response to intracellular bacterial infection. With bacterial contact immediately stimulating host cell surface receptors, it is not surprising that CMPK2 would be induced in response to activation of more central TLR4 signaling that primarily leads to activation of inflammatory programs in the infected macrophages. Moreover, our data of a long-term breakdown of inflammation control in macrophages following prolonged disturbance of CMPK2 expression levels only highlights the importance of rapid and robust regulation of this gene by cells for reverting to basal status. This supports our hypothesis that CMPK2 is an important component of the cellular inflammation rheostat controlling macrophage metabolic and transcriptional response to infections. Pinpointing the precise molecular mechanism of CMPK2 mediated regulation of macrophage immuno-metabolism would help develop novel mechanisms of modulating innate response control paving the way for future host cell directed therapeutics.

Supplementary Figures:

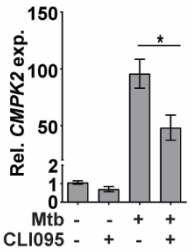

Fig. S1

Fig. S1: Expression of *CMPK2* in THP1 macrophages upon Mtb infection in the presence or absence of CLI095.

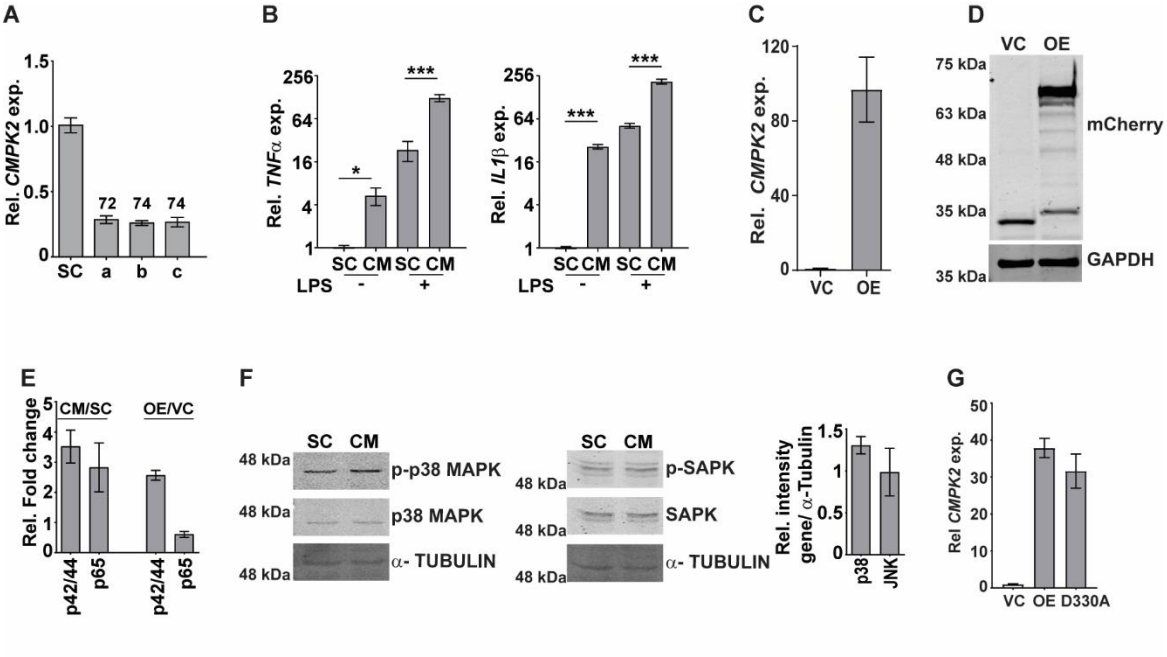

Fig. S2

Fig. S2: A] Expression of *CMPK2* in THP1 macrophages stably expressing the scrambled (SC) siRNA or three different siRNAs (a-c) against CMPK2 by qPCR (B). The gene expression was normalized with *GAPDH* and relative fold changes compared to SC are represented as mean ± SEM (N=2). B] Expression of *TNFα* and *IL1β* gene in SC and CM macrophages following LPS stimulation for 6h. The relative gene expression folds in triplicate assay wells are represented with respect to *GAPDH* as mean ± SEM for N=2.

C] Expression of *CMPK2* in OE or empty vector -VC cells was analyzed by qPCR. The relative gene expression folds in triplicate assay wells are represented with respect to *GAPDH* as mean ± SEM for N=3. D] CMPK2 expression in VC and OE cells were analyzed by immunoblotting with tag specific (mCherry) antibody. E] Relative quantitation of p-ERK and p-NFκB in the SC, CM, VC, OE cells by densitometric analysis of immunoreactivity is shown. Values are mean + SEM of triplicate (N=3) independent blots. F] Analysis of activation of the p38 MAPK and SAPK/JNK signaling pathways in SC and CM macrophages by immunoblotting with antibodies specific for the phosphorylated (active) and non- phosphorylated forms of the proteins. The relative intensities of the blots in the CMPK2 silenced cells w.r.t control (SC) cells are represented as mean ± SEM of N=3. Expression of α-TUBULIN was used as control. G] Expression of *CMPK2* in VC, OE and D330A cells was analyzed by qPCR and is depicted relative to GAPDH levels of N=3 assays.

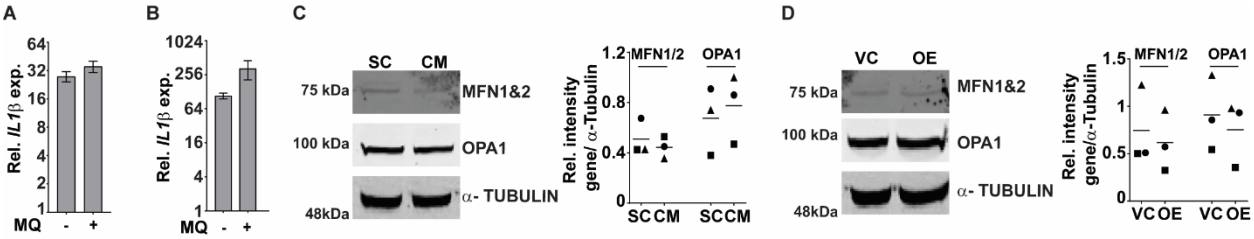

Fig. S3: A, B] Expression of *IL1β* in the macrophages with the addition of a specific mitochondrial ROS inhibitor- MQ at day 2 [A] and day 3 [B] of PMA treatment intervals post activation was analyzed by qPCR. Values are mean fold change in expression with respect to *GAPDH* ± SEM for triplicate assays of N=2/3 experiments. C, D] Expression of proteins involved in mitochondrial fusion by immunoblotting with specific antibodies. MFN1&2 and OPA1 were checked in SC, CM [C] or VC, OE [D] cells along with α-TUBULIN levels as a control. Relative intensity values are depicted ± SEM of N=3.

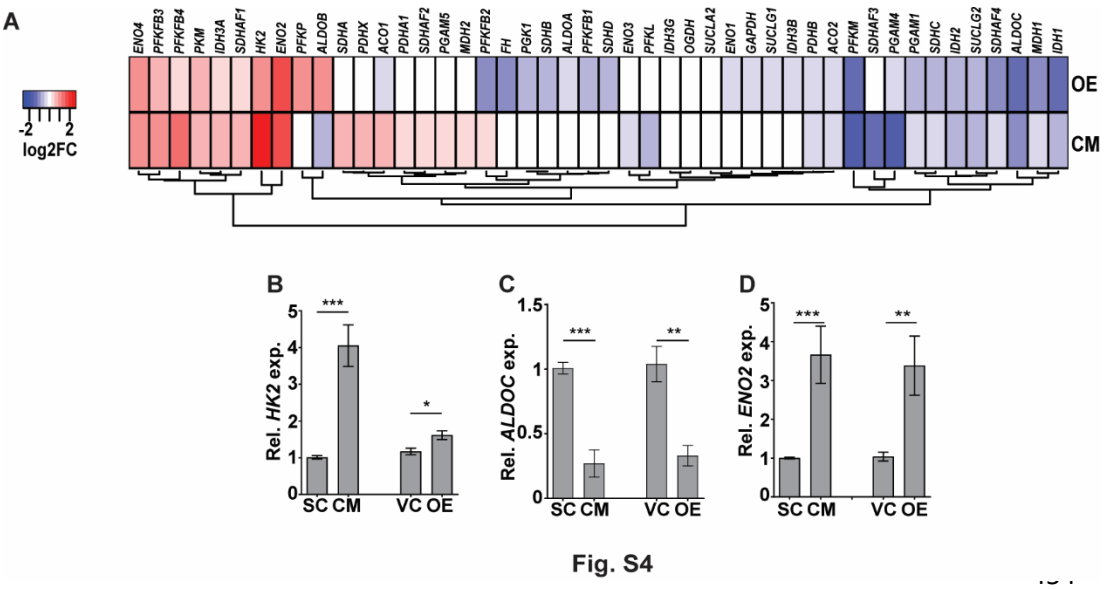

Fig. S4

Fig. S4: A] Expression of genes involved in glycolysis and TCA were represented as heatmap. The expression was extracted from the RNA sequencing data of CMPK2 dysregulated THP1 cell. The values are represented as $\log_2$ compared to respective control cells. B-D] Expression of *HK2* [B], *ALDOC* [C] and *ENO2* [D] was validated by qPCR with specific primers. Values are represented are relative to *GAPDH* expression in the SC, CM, VC and OE cells of N=3 independent assays of triplicate wells.

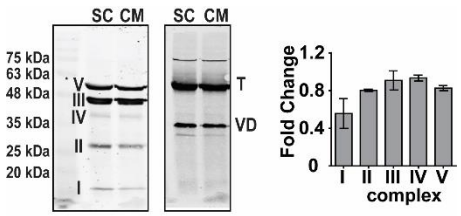

Fig. S5

Fig. S5: Analysis of expression of protein complexes of the mitochondrial respiratory chain in cell lysates of SC and CM macrophages by immunoblotting. α-TUBULIN (T) and VDAC1 (VD) were used as loading controls. The band intensities of the complex proteins were normalized to α-TUBULIN and the relative intensity of CM w.r.t. SC is represented as fold change ± SEM for N=2.

Material and Methods

Reagents

The following chemicals were purchased from Sigma-Aldrich: U0126 (U120), RNAzol RT (R4533), Zymosan (Z4250), Thermo Fisher Scientific: MitoSOX Red (M36008), MitoTracker Deep Red (M22426) and Invivogen: LPS (tlrl-smlps), CLI095 (tlrl-cli095), poly I:C (tlrl-pic), Pam3CSK4 (tlrl-pms). Mitoquinol (89950) was purchased from Cayman Chemical Company.

Cell culture

THP-1 cells were cultured in RPMI-1640 (Himedia laboratories, Mumbai, India) media supplemented with 10% FBS and 1mM sodium pyruvate (Himedia laboratories, Mumbai, India). HEK293T cells were cultured in DMEM supplemented with 10% FBS and 1mM sodium pyruvate. For differentiation, THP-1 cells were treated with 100nM PMA for 24hr and rested for 48hr before the next manipulation. Both cell lines were confirmed for their identity by STR PCR analysis and maintained mycoplasma free by routine checking.

Generation of THP1 lines with CMPK2 silencing

To generate knockdown cells, HEK293T cells were co-transfected with CMPK2 siRNA plasmid (Applied Biological Materials Inc, Richmond, Canada), packaging plasmid (pCMV-dR8.2) and envelope plasmid (pCMV-VSV-G) using Lipofectamine-LTX reagent (Thermo Fisher Scientific India Pvt. Ltd, Mumbai, India). After 6h of transfection, media removed and fresh media was added to the cells. After 48h of transfection, the culture supernatant was collected, centrifuged at 500 rpm to remove cell debris. The virus particles in the supernatant were concentrated to 100µl using Amicon® Ultra-15 Centrifugal Filters (Sigma-Aldrich Chemicals Private Limited, Bengaluru, India) and used to infect THP1 cells. Cells were then selected with 0.6 µg/ml puromycin and GFP positive clones were used for further studies.

Bacterial culturing and infection

Mycobacterium tuberculosis strain Erdman was grown in 7H9 Middlebrook media BD Biosciences, USA) supplemented with Middlebrook ADC (BD, USA) at 37˚C. *E. coli and*

Salmonella enterica serovar Typhimurium were grown in Luria-Bertani (LB) media (Himedia Laboratories, Mumbai, India) at 37°C. Single cell suspension of mid-log phase bacteria was adjusted to the required cell density and then used to infect the differentiated THP-1 macrophages at multiplicity of infection (MOI) of 5. After 6h *p.i.* for Mtb, cells were washed with PBS to remove extracellular bacteria, and at various times post infection, bacterial numbers were enumerated by lysis of cells and plating for CFU in 7H10 agar plates. For *S. typhimurium*/ *E. coli*, post addition of bacteria at a MOI of 10, the plates were centrifuged for 5 min and then left for 20 min at 37°C. The media removed and treated with 100μg/ml of gentamicin for 2h in RPMI at 37°C. The cells were washed with PBS for 3 times, and infection was continued in media containing 12μg/ml of gentamicin and at indicated time points cells were lysed with PBS-Triton-X-100 (1%) for CFU plating on LB agar (Himedia laboratories, Mumbai, India) plates. The colonies were counted and is represented as CFU/well.

Gene expression analysis by qPCR

Total RNA was isolated using RNAzol (Sigma-Aldrich, USA) method and the concentration was quantified using Nanodrop 2000 UV-visible spectrophotometer. cDNA was prepared with 250-1000 ng total RNA by a RT-PCR using Verso cDNA synthesis kit (Thermo Fisher Scientific, USA). qPCR was performed on a Roche LC480 II system using DyNAmo Flash SYBR Green mix (Thermo Fisher Scientific, USA). Primer sequences are given in Table 1.

Cloning of CMPK2 and the D330 variant.

The NFkB promoter from pNFkB-d2GFP was excised by digestion with *Ecl*136II and *Hind*III and the mCherry fragment from pmCherry-N1was removed with *Hind*III and *Hpa*I and ligated to *Nru*I and *Eco*RV digested pcDNA3.1(+) to get the plasmid pPRAM1. The NFkB promoter from pPRAM1 was replaced with EF-1α from pTracer-EF/V5 His A by using *Mlu*I and *Eco*RI to get pPRAM2. The CMPK2 fragments were amplified from THP1 cDNA using the primer sets PP1 and PP2 and cloned into the pPRAM2 using *Kpn*I and *Bam*HI. The D330A catalytic site mutant was

prepared by site directed mutagenesis using the primers PP3 and PP4. The sequences were verified by sequencing. The list of primers used in this study is given in table 1.

Western blotting and ELISA

For immunoblotting, cells were lysed in RIPA buffer, resolved by SDS-PAGE and transferred to nitrocellulose membrane. After blocking with 5% BSA in Tris Buffered Saline Tween (TBST) for 1hr at room temperature, membranes were incubated with the appropriate dilution of the primary antibody overnight, washed with PBS and probed with infra- red dye conjugated secondary antibody and developed in the LI-COR Odyssey platform. The following antibodies were purchased from Cell Signaling Technology: Rabbit anti-α-tubulin (2125), Rabbit anti-phospho-p42/44 (4377), Rabbit anti-p42/44 (4695), Rabbit anti-phospho-NFkB p65 (3033), Rabbit anti-NFkB p65 (4764), Rabbit anti-phospho-JNK (4671), Rabbit anti-JNK (9258), Abcam: Rabbit anti-mCherry (ab167453), Mouse anti-TOM20 (ab56783), Rabbit anti-TIM50 (ab109436), Mouse anti-MFN1/2 (ab57602), Mouse anti-OPA1 (ab194830), Rabbit anti-DRP1 (ab140494), BD Bioscience: Rabbit anti-VDAC (D73D12), Mouse anti-SOD2 (611581) and LI-COR Biotechnology: Goat anti-Rabbit IgG 800 (926-32211), Goat anti-Mouse IgG 680 (926-68070). Rabbit anti-CMPK2 (HPA041430) was purchased from Sigma-Aldrich.

For ELISA, either cell supernatants or cell extracts were used for cytokine estimation with specific kits- TNFα (cat no: 88-7346-77, eBioscience) and IL1β (cat no: 557953, BD Biosciences) ELISA kits according to manufacturer's protocol.

Analysis of ROS by FACS

THP1 monocyte derived macrophages (MDM) were removed with PBS and 4mM EDTA, washed with PBS, resuspended in RPMI media and used for staining with 5µM MitoSOX Red and 100nM MitoTracker Deep Red at 37°C for 30 mins. Cells were then washed twice in HBSS and finally resuspended in 500µl HBSS and analyzed in FACS ARIA II (BD Biosciences).

Metabolite measurement

Intracellular metabolites for MS-based targeted metabolomics were extracted using methanol-water. Briefly, 1.2 x 10^6 cells from each condition were washed three times with ice-cold PBS, and then quenched with methanol-water (4:1). The cell suspension was freeze thawed in liquid nitrogen for three times. The suspension was centrifuged at 15,000 g at 4°C for 10 min. Supernatant was collected, vacuum dried and then reconstituted in 50 µl of 50% methanol. The reconstituted mixture was centrifuged at 15,000 g for 10 min, and 5 µl was injected for LC–MS/MS analysis.

The data were acquired using a Sciex Exion LCTM analytical UHPLC system coupled with a triple quadrupole hybrid ion trap mass spectrometer (QTrap 6500; Sciex) in negative ion mode. Samples were loaded onto an Acquity UPLC BEH HILIC (1.7 µm, 2.1 × 100 mm) column, with a flow rate of 0.3 ml/min. The mobile phases comprising of 10 mM ammonium acetate and 0.1% formic acid (buffer A) and 95% acetonitrile with 5 mM ammonium acetate and 0.1% formic acid (buffer B). The linear mobile phase was applied from 95% to 20% of buffer A. The gradient program was used as follows: 95% buffer B for 1.5 min, 80%–50% buffer B in next 0.5 min, followed by 50% buffer B for next 2 min, and then decreased to 20% buffer B in next 50 s, 20% buffer B for next 2 min, and finally again 95% buffer B for next 2 min. After data acquisition, peaks corresponding to each metabolite were extracted using Sciex Multiquant TM v.3.0 software and the area were exported in an excel sheet. Normalization was performed using total area sum of that particular run.

Oxygen Consumption

3-4 x 10^6 cells of THP1 MDMs in complete RPMI were added to the chambers of the Oxygraphy-2k (O2k, Oroboros Instruments, Innsbruck, Austria). The oxygen concentration was measured over time at 37ºC under constant stirring. The oxygen consumption rate was calculated using XY graph of oxygen consumption and time.

Transcriptome analysis

Total RNA isolated using RNAzol (Sigma Aldrich, India) and transcript sequencing was done commercially by Bencos research solutions private ltd., (Bengaluru, India). cDNA libraries were generated using Truseq RNA Library Prep Kit (Illumina San Diego, USA) and sequenced in a Illumina Novaseq 6000 platform. RNA-seq reads were aligned with hg38 genome using STAR [54]. HTseq-count was used to count the transcripts [55]. The differential expression analysis across samples were analyzed using GSEA [56].

Confocal Microscopy and Image analysis of stained cells

THP1 monocytes (stably transfectants of scrambled or CMPK2 specific siRNA) were transfected with plasmid DNA mtDsRed (kind gift by Dr. Sowmya Sinha Roy, CSIR- IGIB) and selected for stably expressing clones with 400µg/ml of G418. Cells were differentiated on coverslips, fixed with 4% formaldehyde and imaged in a Leica 480 confocal microscopy. For live imaging, monocytes overexpressing CMPK2 were plated at a cell density of 0.3 x 10^6 cells/ml in the cell culture dish containing two chambers per dish (1 ml/ chamber). Mitotracker Green dye was added to the media and the cells were kept in 37ºC CO_2 incubator for 20mins. The cells were imaged on a Leica SP8 confocal microscope.

Mitochondrial localization

Differential centrifugation was employed for mitochondria isolation from the cells [57]. Briefly, 2.5 x 10^6 THP1 MDMs were washed twice with PBS and resuspended in 3 ml ice-cold cell isolation buffer (IBc- containing 10mM Tris pH to 7.4, 1mM EGTA pH to 7.4 and 0.2M sucrose). The cells were homogenized using a glass Teflon pestle potter. The homogenate was then centrifuged at 600g for 10 min at 4ºC, supernatant was collected and centrifuged at 7000g for 10 min at 4ºC. The pellet was then washed and resuspended in 200 µl IB_C and transferred to a 1.5ml Eppendorf tubes. The homogenate was again centrifuged at 7000g for 10 min at 4ºC. The supernatant was discarded and the pellet was resuspended to get the mitochondrial fraction.

For Proteinase K digestion, the mitochondria were resuspended in MS buffer (210mM mannitol, 70mM sucrose, 5mM Tris-HCL-pH 7.5, 1mM EDTA-pH 7.6)/ 20mMHEPES with or without 2

mg/ml Proteinase K (for 15 min) and/or 1% Triton-X-100. The reaction was terminated by addition of 5 mM phenylmethylsulfonyl fluoride. The mixture was centrifuged at 15000g for 15 min and the pellet fraction was collected. For analysis of membrane proteins, the mitochondrial fraction was resuspended in MS buffer with and without 0.1M Na_2CO_3 and incubated in ice for 30 min. The pellet and supernatant fractions were collected 15000g for 15 min. All fraction were analyzed by immunoblotting with respective antibodies.

Graphs and Statistical analysis

Statistical analyses were performed by using the two tailed Student's t-test. GraphPad Prism software was used for graphs and statistical analysis.

Table 1: List of primers used in this study

Name	Primer sequence
CMPK2 F	CCAGGTTGTTGCCATCGAAG
CMPK2 R	CAAGAGGGTGGTGACTTTAAGAG
IL8 F	AGACAGCAGAGCACACAAGC
IL8 R	ATGGTTCCTTCCGGTGGT
GAPDH F	GAAGGTGAAGGTCGGAGTC
GAPDH R	GAAGATGGTGATGGGATTTC
IL1β F	CCTGTCCTGCGTGTTGAAAGA
IL1β R	GGGAACTGGGCAGACTCAAA
TNFα F	CCCCAGGGACCTCTCTCTAATC
TNFα R	GGTTTGCTACAACATGGGCTACA
IP10 F	TCCACGTGTTGAGATCATTGC
IP10 R	GGCCTTCGATTCTGGATTCAG
IL10 F	GCTGGAGGACTTTAAGGGTTACCT
IL10 R	CTTGATGTCTGGGTCTTGGTTCT
VEGFα F	CTGCTGTCTTGGGTGCATTG
VEGFα R	CCATGAACTTCACCACTTCG
PP1	ATGGTACCATGGCCTTCGCCCGCCGGCTC
PP2	CGTCTAGAGGATCCGCCGGTTCACTAAAACTATTCTGG
PP3	CAAATCTCCTGTGATTGTAGCCAGGTACTGGCACAGCAC
PP4	GTGCTGTGCCAGTACCTGGCTACAATCACAGGAGATTTG

Acknowledgements: The authors thank CSIR (VR-BSC0123, MLP2012), and DBT (SG-GAP0088) funding agency for supporting the study. The authors thank Mr. Manish Kumar and

CSIR- BSC0403 for the confocal microscopy facility, CSIR-STS0016 for BSL3 facility. The authors wish to thank Dr. Sowmya Sinha Roy, CSIR-IGIB for the plasmid pmtDsRed. The authors thank PA's doctoral advisory committee members for useful discussions and comments on the project. The mass spectrometry facilities are duly acknowledged. The student fellowships from CSIR: PA-CSIR- SRF, RA, PA- CSIR-BSC0124, MC- CSIR-JRF, India.

Author Contributions: PA, SR, SG, and VR were involved in conceptualizing and design of the work. Experiments was performed by PA, MC, TR and DS. PA and RC performed Mass spectrometry, PA, SG, and VR wrote the manuscript.

Conflict of interest: The authors do not have any competing interests.

References

1. Labbe K, Murley A, Nunnari J. Determinants and functions of mitochondrial behavior. *Annu Rev Cell Dev Biol* **30**, 357-391 (2014).

2. Picard M, McEwen BS. Psychological Stress and Mitochondria: A Conceptual Framework. *Psychosom Med* **80**, 126-140 (2018).

3. Weinberg SE, Sena LA, Chandel NS. Mitochondria in the regulation of innate and adaptive immunity. *Immunity* **42**, 406-417 (2015).

4. Rambold AS, Pearce EL. Mitochondrial Dynamics at the Interface of Immune Cell Metabolism and Function. *Trends Immunol* **39**, 6-18 (2018).

5. Kikuchi Y, Miyauchi M, Iwano I, Kita T, Oomori K, Kizawa I. Adjuvant effects of prostaglandin D2 to cisplatin on human ovarian cancer cell growth in nude mice. *Eur J Cancer Clin Oncol* **24**, 1829-1833 (1988).

6. Newsholme P, Curi R, Gordon S, Newsholme EA. Metabolism of glucose, glutamine, long-chain fatty acids and ketone bodies by murine macrophages. *Biochem J* **239**, 121-125 (1986).

7. Blagih J, Jones RG. Polarizing macrophages through reprogramming of glucose metabolism. *Cell Metab* **15**, 793-795 (2012).

8. Rodriguez-Prados JC*, et al.* Substrate fate in activated macrophages: a comparison between innate, classic, and alternative activation. *J Immunol* **185**, 605-614 (2010).

646
647 9. Viola A, Munari F, Sanchez-Rodriguez R, Scolaro T, Castegna A. The Metabolic Signature of
648 Macrophage Responses. *Front Immunol* **10**, 1462 (2019).

649
650 10. Mills EL*, et al.* Succinate Dehydrogenase Supports Metabolic Repurposing of Mitochondria to
651 Drive Inflammatory Macrophages. *Cell* **167**, 457-470 e413 (2016).

652
653 11. Van den Bossche J*, et al.* Mitochondrial Dysfunction Prevents Repolarization of Inflammatory
654 Macrophages. *Cell Rep* **17**, 684-696 (2016).

655
656 12. Kelly B, O'Neill LA. Metabolic reprogramming in macrophages and dendritic cells in innate
657 immunity. *Cell Res* **25**, 771-784 (2015).

658
659 13. Labadarios D*, et al.* Vitamin A in acne vulgaris. *Clin Exp Dermatol* **12**, 432-436 (1987).

660
661 14. Cohen HB, Mosser DM. Extrinsic and intrinsic control of macrophage inflammatory responses. *J*
662 *Leukoc Biol* **94**, 913-919 (2013).

663
664 15. Yan J, Horng T. Lipid Metabolism in Regulation of Macrophage Functions. *Trends Cell Biol* **30**, 979-
665 989 (2020).

666
667 16. Lawrence T, Natoli G. Transcriptional regulation of macrophage polarization: enabling diversity
668 with identity. *Nat Rev Immunol* **11**, 750-761 (2011).

669
670 17. Sugimoto MA, Sousa LP, Pinho V, Perretti M, Teixeira MM. Resolution of Inflammation: What
671 Controls Its Onset? *Front Immunol* **7**, 160 (2016).

672
673 18. Missiroli S, Genovese I, Perrone M, Vezzani B, Vitto VAM, Giorgi C. The Role of Mitochondria in
674 Inflammation: From Cancer to Neurodegenerative Disorders. *J Clin Med* **9**, (2020).

675
676 19. Tiku V, Tan MW, Dikic I. Mitochondrial Functions in Infection and Immunity. *Trends Cell Biol* **30**,
677 263-275 (2020).

678
679 20. Wang Y, Li N, Zhang X, Horng T. Mitochondrial metabolism regulates macrophage biology. *J Biol*
680 *Chem* **297**, 100904 (2021).

681
682 21. Boxx GM, Cheng G. The Roles of Type I Interferon in Bacterial Infection. *Cell Host Microbe* **19**, 760-
683 769 (2016).

684

685 22. McNab F, Mayer-Barber K, Sher A, Wack A, O'Garra A. Type I interferons in infectious disease. *Nat*
686 *Rev Immunol* **15**, 87-103 (2015).

687
688 23. Kovarik P, Castiglia V, Ivin M, Ebner F. Type I Interferons in Bacterial Infections: A Balancing Act.
689 *Front Immunol* **7**, 652 (2016).

690
691 24. Zhong Z*, et al.* New mitochondrial DNA synthesis enables NLRP3 inflammasome activation. *Nature*
692 **560**, 198-203 (2018).

693
694 25. Xu Y, Johansson M, Karlsson A. Human UMP-CMP kinase 2, a novel nucleoside monophosphate
695 kinase localized in mitochondria. *J Biol Chem* **283**, 1563-1571 (2008).

696
697 26. Suski JM, Lebiedzinska M, Bonora M, Pinton P, Duszynski J, Wieckowski MR. Relation between
698 mitochondrial membrane potential and ROS formation. *Methods Mol Biol* **810**, 183-205 (2012).

699
700 27. Vyssokikh MY*, et al.* Mild depolarization of the inner mitochondrial membrane is a crucial
701 component of an anti-aging program. *Proc Natl Acad Sci U S A* **117**, 6491-6501 (2020).

702
703 28. Martinez FO, Gordon S, Locati M, Mantovani A. Transcriptional profiling of the human monocyte-
704 to-macrophage differentiation and polarization: new molecules and patterns of gene expression.
705 *J Immunol* **177**, 7303-7311 (2006).

706
707 29. Gong T, Liu L, Jiang W, Zhou R. DAMP-sensing receptors in sterile inflammation and inflammatory
708 diseases. *Nat Rev Immunol* **20**, 95-112 (2020).

709
710 30. Mosser DM, Hamidzadeh K, Goncalves R. Macrophages and the maintenance of homeostasis. *Cell*
711 *Mol Immunol* **18**, 579-587 (2021).

712
713 31. Krenkel O, Tacke F. Liver macrophages in tissue homeostasis and disease. *Nat Rev Immunol* **17**,
714 306-321 (2017).

715
716 32. Watanabe S, Alexander M, Misharin AV, Budinger GRS. The role of macrophages in the resolution
717 of inflammation. *J Clin Invest* **129**, 2619-2628 (2019).

718
719 33. Oishi Y, Manabe I. Macrophages in inflammation, repair and regeneration. *Int Immunol* **30**, 511-
720 528 (2018).

721
722 34. Wynn TA, Chawla A, Pollard JW. Macrophage biology in development, homeostasis and disease.
723 *Nature* **496**, 445-455 (2013).

724

725 35. Lavin Y, Mortha A, Rahman A, Merad M. Regulation of macrophage development and function in
726 peripheral tissues. *Nat Rev Immunol* **15**, 731-744 (2015).

727
728 36. Galvan-Pena S, O'Neill LA. Metabolic reprograming in macrophage polarization. *Front Immunol* **5**,
729 420 (2014).

730
731 37. Tan Z*, et al.* Pyruvate dehydrogenase kinase 1 participates in macrophage polarization via
732 regulating glucose metabolism. *J Immunol* **194**, 6082-6089 (2015).

733
734 38. Wang F*, et al.* Glycolytic Stimulation Is Not a Requirement for M2 Macrophage Differentiation.
735 *Cell Metab* **28**, 463-475 e464 (2018).

736
737 39. Mehta MM, Weinberg SE, Chandel NS. Mitochondrial control of immunity: beyond ATP. *Nat Rev*
738 *Immunol* **17**, 608-620 (2017).

739
740 40. Benmoussa K, Garaude J, Acin-Perez R. How Mitochondrial Metabolism Contributes to
741 Macrophage Phenotype and Functions. *J Mol Biol* **430**, 3906-3921 (2018).

742
743 41. Ramond E, Jamet A, Coureuil M, Charbit A. Pivotal Role of Mitochondria in Macrophage Response
744 to Bacterial Pathogens. *Front Immunol* **10**, 2461 (2019).

745
746 42. Ubanako P, Xelwa N, Ntwasa M. LPS induces inflammatory chemokines via TLR-4 signalling and
747 enhances the Warburg Effect in THP-1 cells. *PLoS One* **14**, e0222614 (2019).

748
749 43. Vats D*, et al.* Oxidative metabolism and PGC-1beta attenuate macrophage-mediated
750 inflammation. *Cell Metab* **4**, 13-24 (2006).

751
752 44. Kolliniati O, Ieronymaki E, Vergadi E, Tsatsanis C. Metabolic Regulation of Macrophage Activation.
753 *J Innate Immun*, 1-17 (2021).

754
755 45. El-Diwany R*, et al.* CMPK2 and BCL-G are associated with type 1 interferon-induced HIV restriction
756 in humans. *Sci Adv* **4**, eaat0843 (2018).

757
758 46. Lai JH*, et al.* Mitochondrial CMPK2 mediates immunomodulatory and antiviral activities through
759 IFN-dependent and IFN-independent pathways. *iScience* **24**, 102498 (2021).

760
761 47. Liu W*, et al.* Identification of fish CMPK2 as an interferon stimulated gene against SVCV infection.
762 *Fish Shellfish Immunol* **92**, 125-132 (2019).

763

764 48. Lai JH, Hung LF, Huang CY, Wu DW, Wu CH, Ho LJ. Mitochondrial protein CMPK2 regulates IFN
765 alpha-enhanced foam cell formation, potentially contributing to premature atherosclerosis in SLE.
766 *Arthritis Res Ther* **23**, 120 (2021).

767
768 49. Huang X, Li Y, Fu M, Xin HB. Polarizing Macrophages In Vitro. *Methods Mol Biol* **1784**, 119-126
769 (2018).

770
771 50. Wang P*, et al.* Both decreased and increased SRPK1 levels promote cancer by interfering with
772 PHLPP-mediated dephosphorylation of Akt. *Mol Cell* **54**, 378-391 (2014).

773
774 51. Ó Maoldomhnaigh C*, et al.* Lactate Alters Metabolism in Human Macrophages and Improves Their
775 Ability to Kill Mycobacterium tuberculosis. *Frontiers in Immunology*, 4104 (2021).

776
777 52. Ravanelli S, den Brave F, Hoppe T. Mitochondrial Quality Control Governed by Ubiquitin. *Front*
778 *Cell Dev Biol* **8**, 270 (2020).

779
780 53. Wrobel L*, et al.* Mistargeted mitochondrial proteins activate a proteostatic response in the
781 cytosol. *Nature* **524**, 485-488 (2015).

782
783 54. Dobin A*, et al.* STAR: ultrafast universal RNA-seq aligner. *Bioinformatics* **29**, 15-21 (2013).

784
785 55. Anders S, Pyl PT, Huber W. HTSeq--a Python framework to work with high-throughput sequencing
786 data. *Bioinformatics* **31**, 166-169 (2015).

787
788 56. Subramanian A*, et al.* Gene set enrichment analysis: a knowledge-based approach for interpreting
789 genome-wide expression profiles. *Proc Natl Acad Sci U S A* **102**, 15545-15550 (2005).

790
791 57. Frezza C, Cipolat S, Scorrano L. Organelle isolation: functional mitochondria from mouse liver,
792 muscle and cultured fibroblasts. *Nat Protoc* **2**, 287-295 (2007).

793

794

795